Materials and Structures/Matériaux et Constructions, Vol. **30**, October 1997, pp 486-496

SCIENTIFIC REPORTS

Strengthening of historic masonry structures with composite materials

Thanasis C. Triantafillou, Michael N. Fardis
Dept. of Civil Engineering, University of Patras, Patras 26500, Greece

Paper received: April 25, 1996; Paper accepted: June 18, 1996

ABSTRACT

This paper deals with the application of unidirectional fibre-reinforced polymer tendons for the reversible strengthening of masonry monuments. The tendons, anchored to the masonry only at the ends, are circumferentially applied on the external face of the structure and post-tensioned to provide horizontal confinement. The relevant properties of fibre-reinforced polymer materials and prestressing systems are summarised; in addition, the concepts for their application, including anchorage, to masonry structures are developed, and a general design procedure is presented. The effectiveness of the strengthening technique is established both analytically, for structures with simple geometries, and numerically, for a real three-dimensional structure with openings, based on the finite element method. The effects of temperature changes on the tendons and the masonry are shown to be negligible. It is concluded that the effectiveness of the proposed method in the consolidation of historic masonry structures is quite satisfactory, especially when the strengthening elements are made of carbon fibre-reinforced polymer.

RÉSUMÉ

Cet article présente l'utilisation de câbles unidirectionnels en polymère renforcé de fibres pour le renforcement réversible des monuments en maçonnerie. Les câbles, ancrés dans la maçonnerie uniquement aux extrémités, sont appliqués de manière circonférentielle sur la face externe de la structure et précontraints pour fournir un confinement horizontal. On résume les propriétés des matériaux polymères renforcés de fibres et les systèmes de précontrainte. Les concepts pour leur application, y compris l'ancrage, aux constructions en maçonnerie sont discutés, et une procédure générale de conception est présentée. L'efficacité de la technique de renforcement est établie à la fois analytiquement, pour des constructions à géométrie simple, et numériquement, pour de véritables constructions à trois dimensions ayant des ouvertures, sur la base de la méthode des éléments finis. Il est montré que les effets des variations de température sur les câbles et sur la maçonnerie sont négligeables. On conclut que l'efficacité de la méthode proposée pour la consolidation des constructions historiques en maçonnerie est tout à fait satisfaisante, surtout lorsque les éléments de renforcement sont constitués de polymère renforcé de fibres en carbone.

1. INTRODUCTION

In recent years, the importance of structural interventions in the area of architectural heritage (monuments, historic buildings and bridges, etc.) for repair and strengthening has increased considerably. Such interventions often follow special guidelines, *e.g.* those of the Charter of Venice [1]. Very significant among these guidelines are the requirements that these interventions should not adversely affect the *character* of the monument and must be *reversible*, especially when the techniques applied have not been proven by very long in-service performance records. Among the methods used to upgrade historic structures are: (a) filling of cracks and voids using grout injections; (b) stitching of large cracks and other weak areas with metallic or brick elements or concrete zones; (c) application of reinforced grouted perforations to improve the cohesion and tensile strength of masonry; (d) external jacketing by shotcrete or by cast-in-situ concrete; and (e) external or internal post-tensioning with steel ties, in order to tie structural elements together into an integrated three-dimensional system [2-3].

Unlike other methods, external post-tensioning with steel ties combines efficiency, simplicity and reversibility. It has been applied on many historic structures, such as: the Rotunda and the San Andreas domes in Thessaloniki, Greece [2]; the Martinego rampart of the Old Castle in Corfu, Greece [4]; the Pisa Tower, strengthened through

Editorial note
Prof. Thanasis Triantafillou is a RILEM Senior Member.

circumferentially-applied zinc-coated galvanised steel tendons placed inside plastic tubes to provide further corrosion resistance [5]; the domes of St. Ignatius of Loyola in Spain [6] and the St. Charles Basilica in Rome [7] using circumferential stainless steel cables; and the external walls of the St. Mary of the Angels Basilica in Assisi, using polyethylene tendons placed inside the masonry walls [6].

Post-tensioning with steel ties presents several practical difficulties in protecting the strands against corrosion and other environmental effects, and sometimes in their handling at the construction site (due to their considerable weight). To overcome durability problems, designers have to select prestressing elements with large diametres, thus violating the basic principles of aesthetics. As an alternative, the steel ties can be replaced with advanced fibre-reinforced polymer (FRP) materials, commonly called composites, which offer excellent physical and mechanical properties and are lightweight and insensitive to corrosion. Such ties may be applied to historic structures in a reversible manner, in the form of external tendons in a colour which matches that of the external surface of the structure, as first proposed in [8].

In this paper, the authors establish the applicability of composite materials in the strengthening of masonry-type monuments. The relevant properties of these materials are summarised, the concepts for their application in masonry structures are presented (including attachment), and a design procedure is proposed. Next, the effectiveness of the strengthening technique is established both analytically (for structures with simple geometries) and numerically (for a real three-dimensional structure with openings, based on the finite element method). Finally, the effects of temperature changes on the tendons and on the masonry are studied, and a brief discussion on the optimum selection of FRP materials suitable for the proposed application is provided.

2. COMPOSITES AS STRENGTHENING MATERIALS

Fibre-reinforced polymers (FRP) have been used extensively in a variety of industries, including aerospace, automotive, ship-building and sports. They are becoming increasingly important in the construction industry as well, with great potential in many areas, thereby offering the designer an outstanding combination of properties not available from other materials. Glass, aramid or carbon fibres (with diametres in the range of 5-25 μm) can be introduced within a certain position, volume and direction in a binding matrix (*e.g.* epoxy, polyester, vinylester) for maximum efficiency. When the fibres are continuous, parallel and at high volume fractions (typically more than 50%), a unidirectional material is produced with a strength and stiffness close to those of the fibres and with the chemical resistance of the matrix [9]. Among the other properties they provide, unidirectional composites offer high strength and stiffness, lightness and insensitivity

Table 1 – Typical FRP post-tensioning systems and associated properties (according to manufacturers)

Product	Fibre/ matrix	Fibre volume fraction (%)	Density (kg/m^3)	Coeff. of thermal expansion ($\times 10^{-6}$/°C)	Elastic modulus (GPa)	Tensile strength (GPa)	Ultim. tensile strain (%)	Poisson's ratio (-)	Creep/ elastic strain	Relaxation (%)	Stress rupture[3]
Polystal	E-Glass/ polyester	68	2000	7.0	51	1.57	3.3	0.27	0.03 (2 yrs)	1.4 (100 hrs) 3.5 (100 yrs)[5]	0.70[4]
Parafil G	Aramid (Kevlar 49)	100	1400	-5.7	120	1.95	1.6		0.04 (1 day)	4.0 (100 hrs) 8.0 (100 yrs)	0.40
Arapree	Aramid (Twaron)/ epoxy	44	1400	-1.8	55	1.35	2.4	0.38	0.002[2] (100 yrs)	7.5 (100 hrs) 15 (100 yrs)	0.60
FiBRA	Aramid (Kevlar 49)/ epoxy[1]	65	1300		64	1.35	2.2	0.62		10 (100 hrs) 20 (100 yrs)	
Teijin	Aramid (Technora)/ vinylester	65	1300		55	1.90	3.6	0.35		8 (100 hrs) 20 (100 yrs)	
CFCC	Carbon (Besfight)/ epoxy	60	1500	0.6	137	1.80	1.6		0.0004 (100 hrs, 180 °C)	1 (100 hrs)	
Leadline	Carbon (Dialead)/ epoxy	65	1600		147	1.80	1.3				

[1] *Braided Aramid, impregnated with epoxy.*
[2] *This value appears to be low for AFRP, which creeps considerably more than GFRP and CFRP.*
[3] *Projected residual strength as a fraction of the short-term strength, after stressing the elements at about 50% of the short-term strength for 100 yrs (and testing after unloading).*
[4] *This value appears to be too high for glass/polyester, which displays poor stress rupture behaviour.*
[5] *Extrapolated value, according to manufacturers.*

to corrosion. Therefore, use of these materials for special applications in construction is highly attractive and cost-effective due to improved durability, reduced life-cycle maintenance costs, savings from easier transportation and improved on-site productivity.

Because of their advantages over conventional materials (low and high strength steels), unidirectional FRPs have found their way into numerous construction applications, including: (a) development of prestressing tendons, *e.g.* [10-18]; and (b) strengthening of concrete, *e.g.* [19], wood, *e.g.* [20-21] and masonry, *e.g.* [22-23], structures with non-prestressed or sometimes prestressed laminates, bonded externally to the tension faces using epoxy adhesives. In most of these applications, the composites are manufactured by highly-automated processes such as pultrusion, in which fibres are pulled through a heated die into which resin is injected, and a fully-cured element is produced with good dimensional stability.

The concept described and analysed here for the application of advanced composites as strengthening materials of masonry-type historic structures involves the introduction of horizontal circumferential, externally-attached post-tensioned ties. There is quite a large number of manufacturers and suppliers of post-tensioned FRP materials around the world, and several companies provide complete tendon-anchorage systems. Basic information about some of the widely-known FRP post-tensioning systems is given in Table 1, *e.g.* [10-18].

Composites are often subjected to environmental effects such as attack by chemicals, moisture uptake, temperature fluctuations and irradiation with ultra-violet light (UV), which may lead to deterioration and premature failure. In general, carbon fibre-reinforced polymers (CFRP) are highly resistant to these effects; glass fibre-reinforced polymers (GFRP) are sensitive, and aramid fibre-reinforced polymers (AFRP) display an intermediate behaviour. The detrimental action of moisture and chemicals (*e.g.* alkalis) on GFRP, and that of UV on AFRP, deserve special mention. Finally, it is also worth mentioning that in some of the prestressing systems above, the rods are protected: in Polystal, a 0.5-mm polyamide coating is employed; in Parafil G, the continuous fibres are contained within a thermoplastic sheath; and in CFCC, the wires are overwrapped with a polymeric yarn.

3. CONCEPTS AND ANCHORAGE

Masonry structures can be consolidated and strengthened using circumferential FRP tendons. The tendons, in the form of either round rods or strips attached to the masonry only at their ends, are circumferentially applied on the external face of the structure and post-tensioned to provide horizontal confinement. Due to their anisotropic nature, unidirectional composites have relatively low transverse compressive strength (on the order of 10% of their tensile strength in the strong direction) and even lower (interlaminar) shear strength. Furthermore, because of their brittle nature, the materials are sensitive to stress concentrations and hence cannot be pierced or threaded.

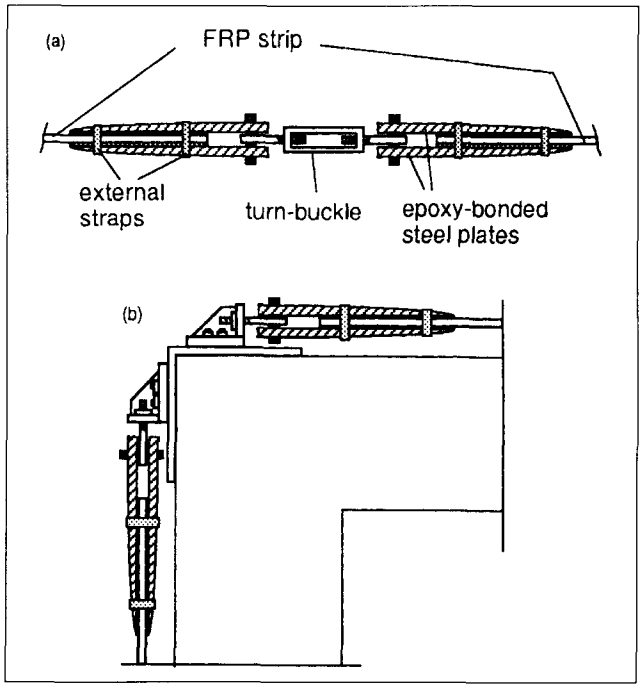

Fig. 1 – Proposed FRP anchorage/attachment: (a) for circumferential prestressing of circular domes; and (b) at masonry corners.

Finally, their abrasion resistance allows only limited frictional stresses. Thus, conventional anchoring solutions (upset heads, threads, wedges, etc.) are not applicable, and relatively large anchor lengths are required. Strip-like tendons are better than round ones for the external post-tensioning of masonry, because they minimise anchor lengths (due to their large surface area) and simplify the attachment of anchorages on the masonry. Proposed concepts for anchorages and their (reversible) attachment are illustrated in Fig. 1.

Fig. 1a refers to the circumferential prestressing of structures with a circular plan and involves a single FRP tendon around the perimetre, gripped at each end between stainless steel plates to which it is epoxy-bonded (note that the epoxy adhesive is not exposed, so that durability is not of major concern). Improved attachment of the tendon to the plates is achieved by clamping through external straps, which introduce transverse compression to both the adhesive and the FRP, thus increasing their strength and minimising creep in the adhesive. Each pair of plates is connected to a usual threaded bar coupler (turn-buckle) through a threaded stainless steel bar.

Because FRP tendons cannot be bent to a large curvature, they cannot turn around sharp corners of the structure and have to be individually anchored. For this latter case, the anchorage in Fig. 1b is proposed herein, involving a structural stainless steel angle not permanently attached to the corner of the wall and transferring prestressing forces to the masonry through contact forces. The two tendons anchored at the same corner angle have to be prestressed gradually, by alternate turning of the nuts at their end anchorage, so that at each corner the moments of the individual tendon forces with respect to the corresponding wall mid-surface counterbalance each other. Note that the FRP tendons could also turn around

masonry corners provided that: (a) an appropriate radius of curvature R_w is selected so that the additional strain, $t_{frp}/2R_w$ (t_{frp} = thickness of tendon), is a small fraction of the FRP failure strain, and (b) the friction coefficient of the contact area at the corner is small.

4. GENERAL REDESIGN/STRENGTHENING PROCEDURE

The procedure described next for proportioning the post-tensioned FRP tendons follows the partial-safety-factor safety format for the Ultimate Limit State (ULS), as advocated by the Joint Committee for Structural Safety and adopted in the system of Eurocodes.

Considering that at the generic point **x** of the structure the masonry is in a biaxial state of stress, the strengthening effect of circumferential prestressing by FRP is due to the beneficial effect of introducing additional compression into each normal stress component. If the ultimate strength (or ULS) condition of the masonry, shown in Fig. 2 in biaxial principal stress space for the case of isotropic stone masonry (typically found in old masonry structures), is expressed as:

$$f(\boldsymbol{\sigma}(\mathbf{x})) - r(\mathbf{x}) = 0 \quad (1)$$

in which for biaxial stresses $\boldsymbol{\sigma}$ stands for (σ_1, σ_2) or, in general, for (σ_x, σ_y, τ_{xy}) for anisotropic (*e.g.* brick) masonry, then the ULS verification condition under biaxial stresses becomes the following:

$$f\left(\boldsymbol{\sigma}(\mathbf{x})\right) - r_d(\mathbf{x}) \equiv f\left(\boldsymbol{\sigma}(\mathbf{x})\right) - \frac{r(\mathbf{x})}{\gamma_w} \le 0 \quad (2)$$

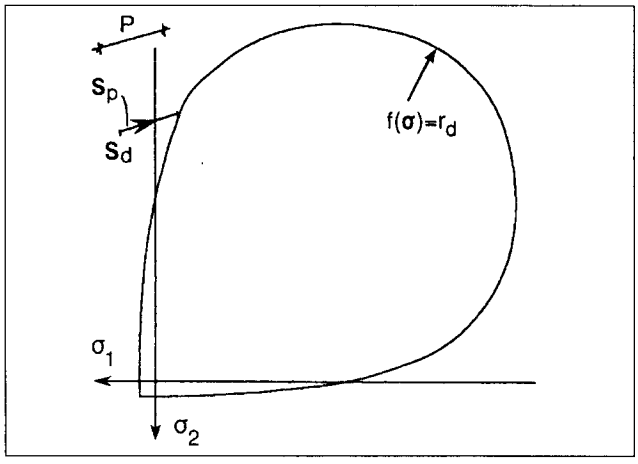

Fig. 2 – Schematic design procedure in biaxial stress space.

In (1) and (2), the "constant" r(**x**) of the ultimate strength condition is a measure of the as-built strength of the masonry, *e.g.* its uniaxial compressive strength in the horizontal or vertical direction, and depends, in general, on location **x**. γ_w in (2) is the material partial safety factor for old masonry, which may be different from the one for new masonry (its value may be taken as higher, due to the historical importance of the structure, or lower, due to greater knowledge of the as-built strength properties).

As proposed in [24], the ultimate strength condition of isotropic masonry under triaxial stress conditions can be fitted by the triaxial failure criterion proposed in [25] for concrete:

$$\alpha J_2 + \lambda\sqrt{J_2} + \beta I_1 = 1 \quad (3)$$

in which I_1 is the first stress invariant, J_2 is the second deviatoric stress invariant and λ is given by:

$$\lambda = c_1 \cos\frac{\cos^{-1}(c_2 \cos 3\theta)}{3} \quad \text{if} \quad \cos 3\theta \ge 0 \quad (4a)$$

$$\lambda = c_1 \cos\left(\frac{\pi - \cos^{-1}(-c_2 \cos 3\theta)}{3}\right) \quad \text{if} \quad \cos 3\theta < 0 \quad (4b)$$

In (4a, b), $\cos\theta$ is given by:

$$\cos 3\theta = \frac{3\sqrt{3}\ J_3}{2J_2^{3/2}} \quad (5)$$

where J_3 is the third deviatoric stress invariant. To fit biaxial test data for stone masonry with a ratio of uniaxial strengths in tension and compression equal to 0.085 and with a ratio of equal biaxial-to-uniaxial compression strength equal to 1.65, the following parametre values are proposed in [24]:

$$\alpha = \frac{0.665}{f_w^2} \quad \beta = \frac{3.84}{f_w} \quad c_1 = \frac{13.8}{f_w} \quad c_2 = 0.959 \quad (6)$$

where f_w = uniaxial compressive strength of masonry. For anisotropic (brick) masonry, models such as that presented in [26] including tensile strength of bed joints, or those proposed in [27] or [28], may be used.

The state of stress in (1) and (2) equals:

$$\boldsymbol{\sigma}(\mathbf{x}) = \mathbf{S}_d(\mathbf{x}) + \sum_{i=1,\ n_p} P_i\, \mathbf{S}_{pi}(\mathbf{x}) \quad (7)$$

in which $\mathbf{S}_d(\mathbf{x})$ is the value of $\boldsymbol{\sigma}(\mathbf{x})$ due to the ULS design combination of actions, factored with the appropriate load partial safety factors, γ_F, and combination factors, ψ_0. P_i is the unknown value of the prestressing force of the FRP tendon or group of tendons i; $\mathbf{S}_{pi}(\mathbf{x})$ is the state of stress at **x** due to $P_i = 1$ and n_p is the number of tendons or groups of tendons with independently distinct and unknown prestress force values. For simple geometries, such as rectangular in plan structures or spherical domes, analytical expressions for the stresses $\mathbf{S}_d(\mathbf{x})$ and $\mathbf{S}_{pi}(\mathbf{x})$ can be obtained, while for complicated three-dimensional structures with openings in the walls, finite element analyses are required.

The n_p unknown prestressing forces are determined by satisfying the nonlinear in these values ULS verification condition, (2), at n_p representative locations **x**. Alternatively, we may seek to minimise a linear functional of P_i, which expresses the total cost of prestressing, subject to the nonlinear constraints:

$$f(\boldsymbol{\sigma})(\mathbf{x})) - r_d(\mathbf{x}) \le 0 \quad (8)$$

at more than n_p locations **x**.

Normally in good approximation, the state of stress within an area of the structure is affected only by the

value P of the prestressing force of a single group of FRP tendons, typically located within the same area:

$$\boldsymbol{\sigma}(\mathbf{x}) \approx \mathbf{S}_d(\mathbf{x}) + P\,\mathbf{S}_p(\mathbf{x}) \tag{9}$$

The meaning of the combination of (2) and (9) is shown in Fig. 2. P is the distance of the stress point $\mathbf{S}_d(\mathbf{x})$ due to the design actions from the design ULS condition, (2), measured along the direction defined by the stress vector $\mathbf{S}_p(\mathbf{x})$ through the point $\mathbf{S}_d(\mathbf{x})$. The problem of determination of P has a solution only if the arrangement of tendons is such that the line through $\mathbf{S}_d(\mathbf{x})$ along the direction of $\mathbf{S}_p(\mathbf{x})$ intersects the design ULS condition, (2).

Once the values of the P_i have been determined, the cross-sections of the tendons are computed on the basis of the FRP material design strength, $f_{frp,d} = f_{frp,k} / \gamma_{frp}$, where $f_{frp,k}$ is the characteristic tensile strength of the FRP material multiplied by an FRP strength reduction factor, α_s, due to sustained loading [see (13) below]. The value of the material partial safety factor γ_{frp} (which would be equal to 1.15 for steel tendons) depends on the dispersion of the FRP strength as well as on the ratio between its mean and characteristic values, taking into consideration the consequences of its (brittle) failure. For the design of the anchorage by epoxy-bonding and clamping to the plates, the ratio of the anchorage length to the thickness of the FRP strip should (roughly speaking) not be less than one-half the ratio between the design strength values of the FRP in tension and the epoxy in shear. Finally, for the anchorage detail of Fig. 1b, the bearing strength of the masonry should be checked, taking into account the beneficial effect of stress triaxiality under the contact plates.

5. MECHANICAL BEHAVIOUR OF BIAXIALLY LOADED MASONRY - SIMPLE CASES

5.1 Effect of prestressing

Assuming that the state of stress in the strengthened structure is biaxial and that the prestressing forces are distributed so that the FRP tendons can be considered as smeared, the effect of prestressing on the masonry wall is a confining stress σ_{wp} equal to

$$\sigma_{wp} = \sigma_{p\infty}\,\rho_{frp} \tag{10}$$

where $\sigma_{p\infty}$ is the final value of stress in the tendons after losses due to relaxation of the tendons (including that in the anchorages) and creep of the masonry, and ρ_{frp} is the area fraction of FRP material or the reinforcement ratio, that is the ratio of the FRP cross-sectional area to the area of the prestressed masonry.

The final tendon stress $\sigma_{p\infty}$ is computed from the ULS verification condition for the tendons in tension:

$$S_d \le R_d \tag{11}$$

where S_d = design action, given as the product of the final stress in the tendons, $\sigma_{p\infty}$, times γ_p, the partial safety factor for prestressing, equal to 1.2 [29]:

$$S_d = \gamma_p\,\sigma_{p\infty} \tag{12}$$

and R_d = long-term design resistance of the tendons, given as

$$R_d = \alpha_s \frac{f_{frp,k}}{\gamma_{frp}} \tag{13}$$

where α_s = composite material tensile strength reduction factor due to sustained loading ($\alpha_s < 1$ for composite tendons, as opposed to $\alpha_s = 1$ for steel tendons).

Combining (10)-(13), the confining stress σ_{wp} is expressed as:

$$\sigma_{wp} = \frac{\alpha_s}{\gamma_p}\frac{f_{frp,k}}{\gamma_{frp}}\rho_{frp} \tag{14}$$

On the basis of a variety of FRP material properties, the typical values for $f_{frp,k}$, α_s, and γ_{frp} for GFRP, AFRP and CFRP are proposed in Table 2.

The effect of prestressing with FRP tendons will be described next through two simple case studies: a rectangular in plan masonry structure and a semi-spherical dome.

Table 2 - Characteristic FRP strengths and proposed strength reduction and partial safety factors

FRP Material	$f_{frp,k}$ (MPa)	α_s	γ_{frp}
GFRP	1700	0.45	1.25
AFRP	1500	0.55	1.20
CFRP	1900	0.75	1.15

5.2 Rectangular masonry structure

The state of stress in a typical element of a rectangular masonry structure subjected to both vertical and horizontal loading (Fig. 3a) and strengthened with horizontal FRP ties is given in Fig. 3b. This state of stress corresponds to the following stress invariants:

$$I_1 = \sigma_v + \sigma_{wp} \tag{15a}$$

$$J_2 = \frac{1}{3}\left(\sigma_v^2 + \sigma_{wp}^2 - \sigma_v\sigma_{wp} + 3\tau^2\right) \tag{15b}$$

$$J_3 = \frac{1}{3}\left(\sigma_v + \sigma_{wp}\right)\left[\frac{2}{9}\left(\sigma_v + \sigma_{wp}\right)^2 - \sigma_v\sigma_{wp} + \tau^2\right] \tag{15c}$$

where σ_v and τ are the vertical and shear stresses in the masonry due to the design combination of gravity loads and external loading (*e.g.* due to wind or seismic actions).

Substituting (15a)-(15c) into the failure criterion of (3) with the parametre values of (6) gives the combinations of σ_v, σ_{wp} and τ at attainment of the design ULS condition of the masonry. Hence, Fig. 4 is obtained, which provides the maximum shear stress that the strengthened masonry can sustain as a function of the confinement, for various values of the vertical stress. Note that in Fig. 4, all the stresses are normalised with respect to the design strength of masonry in uniaxial compression, f_{wd}. These results are

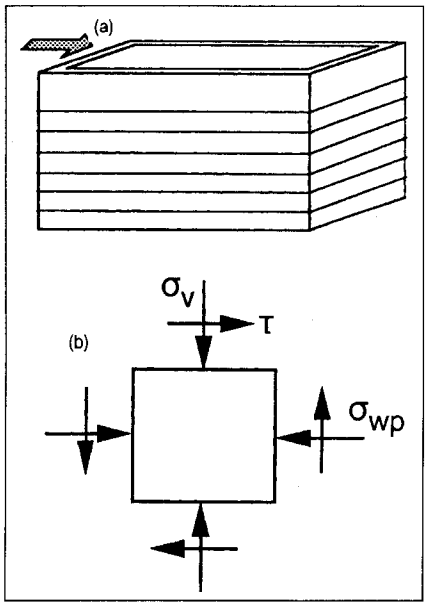

Fig. 3 – (a) Rectangular masonry structure under vertical and horizontal loading; (b) state of stress.

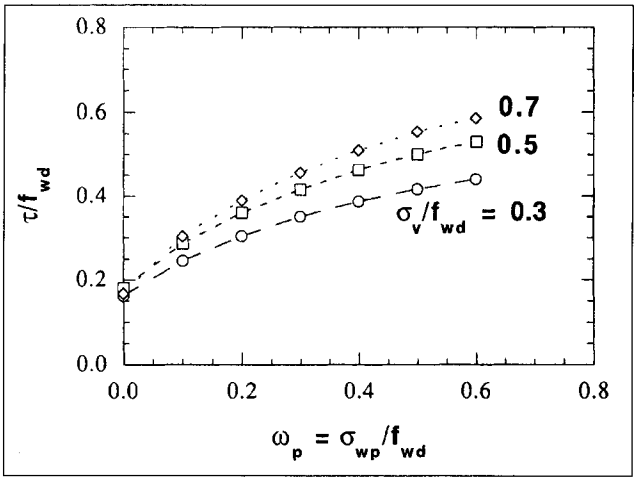

Fig. 4 – Maximum shear stress versus masonry prestress for different vertical stress values.

independent of the prestressing material type and masonry strength, and demonstrate that horizontal prestressing may result in considerable increase in the shear capacity of (isotropic) masonry structures; this beneficial effect becomes more pronounced as the vertical stresses increase.

Next, considering that σ_{wp} is given by (14) (with the values of Table 2), the failure criterion of (3) with the values of (6) can be solved for the maximum shear stress that can be resisted, τ, in terms of ρ_{frp}, for known values of the vertical stress σ_v. The resulting stresses (again normalised with respect to f_{wd}) are given in Fig. 5 for three different composite tendon materials. It is demonstrated that, as expected, the beneficial effect of horizontal confinement increases with the FRP area fraction (and with the vertical stress). Also, the increase in shear resistance is highest when the tendons are made of CFRP, and is approximately the same for GFRP or AFRP. This last statement becomes clearer from the results of Fig. 6, in which the shear resistance is plotted in terms of ρ_{frp} for all three composites and for constant σ_v. Glass and aramid composites are penalised both by the combination of their lower

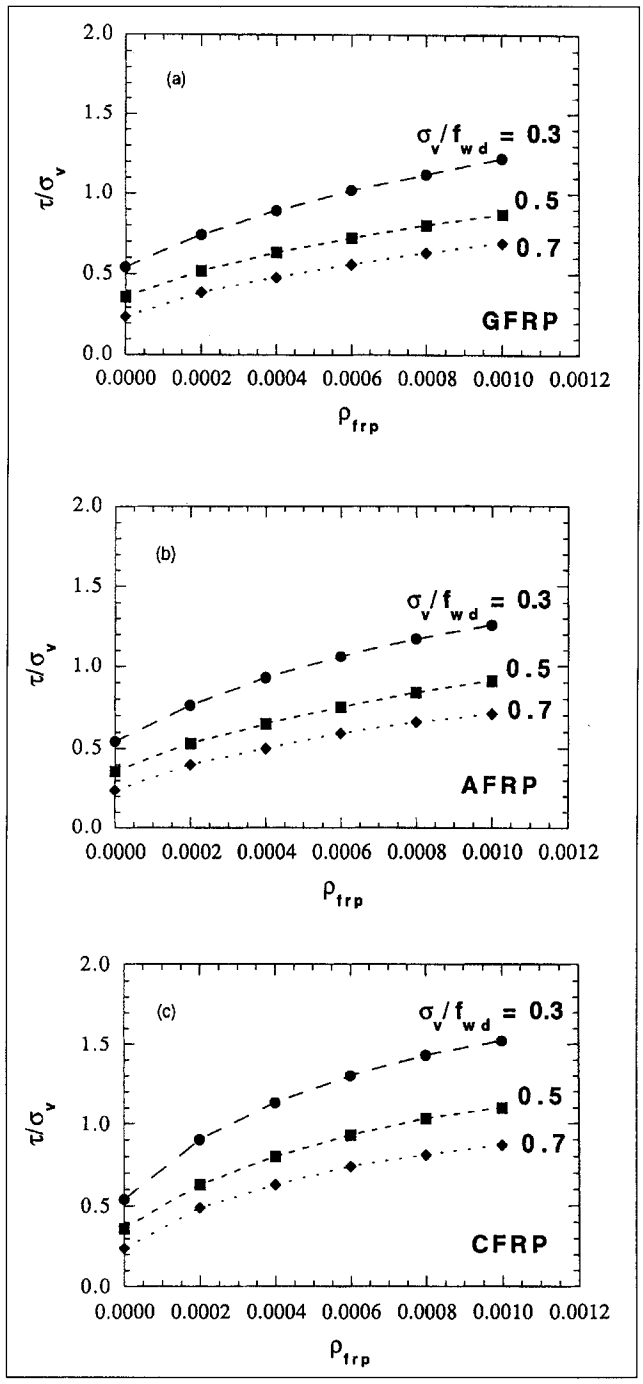

Fig. 5 – Maximum shear stress versus FRP area fraction for different vertical stress values: (a) GFRP; (b) AFRP; and (c) CFRP.

(compared with CFRP) tensile strengths and reduction factors due to sustained loading, and the higher material safety factors required for them due to their larger dispersion of strength values.

5.3 Semi-spherical dome

The analysis for the rectangular structure is repeated for the case of a semi-spherical dome, with radius R and wall thickness t, subjected to a uniformly-distributed vertical loading, with a design value equal to q_d (Fig. 7a). The state of stress in a typical element near the base of the dome

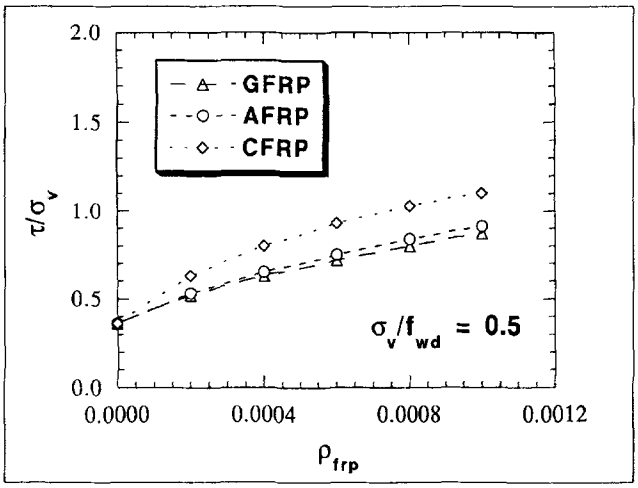

Fig. 6 – Maximum shear stress versus FRP area fraction for a given vertical stress and three types of FRP tendons.

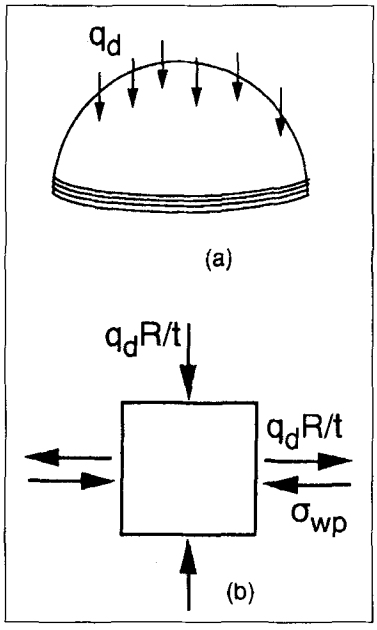

Fig. 7 – (a) Semi-spherical dome under vertical loading; (b) state of stress near the base.

(most critical region) is shown in Fig. 7b and corresponds to the following stress invariants:

$$I_1 = \sigma_{wp} \tag{16a}$$

$$J_2 = \frac{1}{3}\left[\sigma_{wp}^2 + 3\left(q_d\frac{R}{t}\right)^2 - 3\sigma_{wp}\left(q_d\frac{R}{t}\right)\right] \tag{16b}$$

$$J_3 = -\frac{1}{3}\sigma_{wp}\left[\frac{2}{9}\sigma_{wp}^2 + \left(q_d\frac{R}{t}\right)^2 - \sigma_{wp}\left(q_d\frac{R}{t}\right)\right] \tag{16c}$$

Substitution of (16a)-(16c) into the failure criterion of (3) with the parametre values of (6), yields the combinations of q_d and σ_{wp} at failure of the dome near the base. Considering that σ_{wp} is given by (14) (with the values of Table 2), the resulting equation can be solved for the maximum vertical load in terms of ρ_{frp}, for a known value of R/t. The results are shown in Fig. 8 (normalised with respect to f_{wd}), for three different composite tendon materials and for two values of R/t (10 and 15). It is clear that horizontal prestressing near the base of the dome results in considerable increase in the vertical load-bearing capacity of the structure. This beneficial effect increases almost linearly with the FRP area fraction, is almost independent of the R/t ratio and is more pronounced for CFRP tendons. As shown in Fig. 9, these tendons provide an approximately 100% higher increase, in comparison with AFRP or GFRP, for the same FRP area fraction.

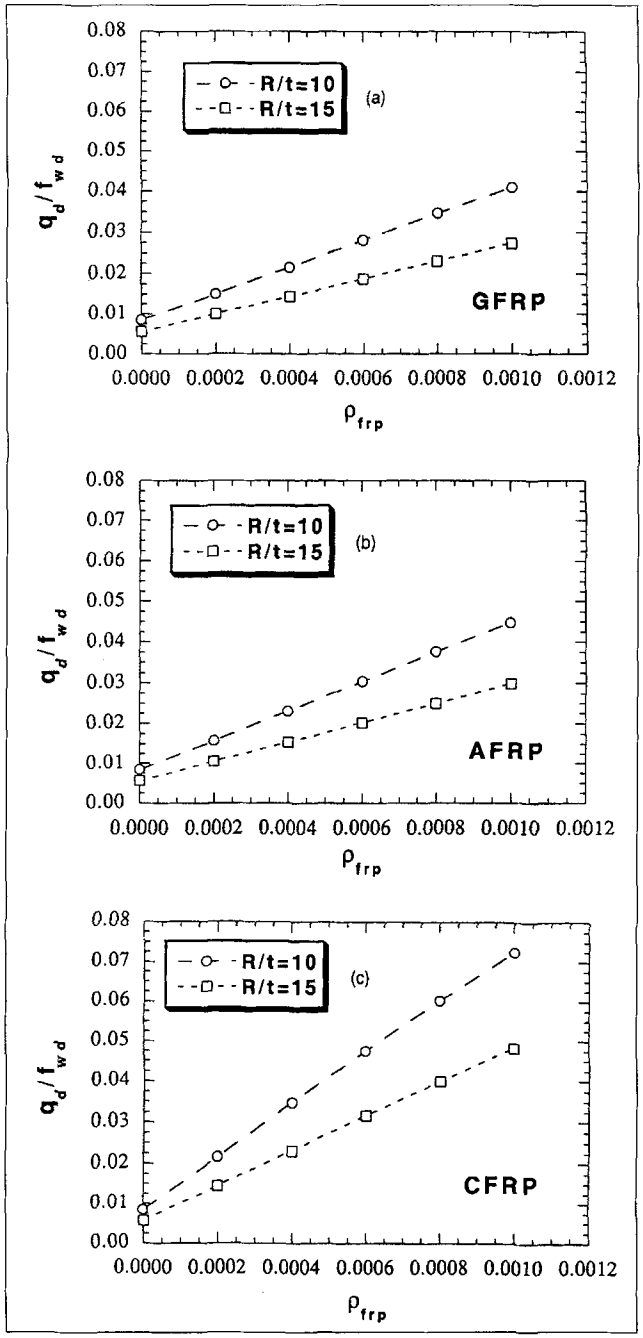

Fig. 8 – Maximum vertical load versus FRP area fraction for two different R/t ratios: (a) GFRP; (b) AFRP; and (c) CFRP.

6. FINITE ELEMENT ANALYSIS OF AN OLD MASONRY BUILDING

This section is devoted to the Finite Element study of the effectiveness of strengthening through horizontal prestressing with FRP tendons. The study refers to a historic masonry building located in Patras, Greece. Each wall of the building was discretised into a large number of four-

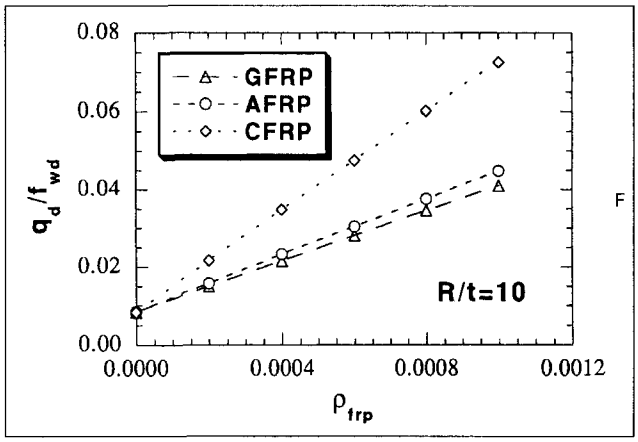

Fig. 9 – Maximum vertical load versus FRP area fraction for a given R/t ratio and three types of FRP tendons.

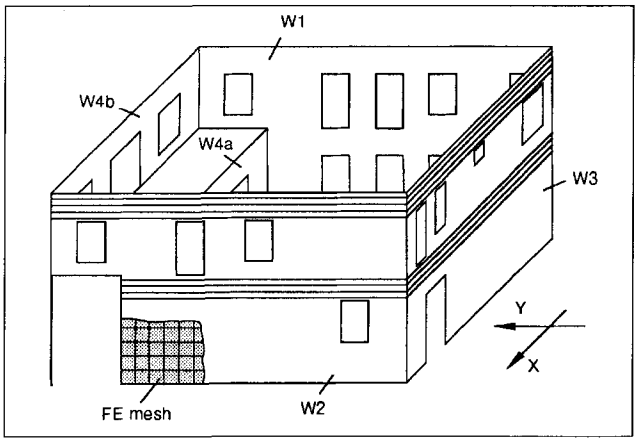

Fig. 10 – Schematic illustration of strengthened masonry building and part of finite element discretisation.

node isoparametric elements (Fig. 10), which are the combination of thick-plate and plane-stress elements. Each node has five degrees of freedom: three displacements and two rotations (the rotation about the normal to the mid-surface is suppressed as an independent DOF). The elements have 3 × 3 Gauss integration, and stress and strain results are obtained at the nodes by surface extrapolation from those at the integration points. Element thickness is equal to that of the wall, 0.6 m, and dimensions within the plane of the wall are about 0.6 m, as required for modelling the geometry around openings. The wood floor and roof were modelled using truss elements in the direction of the joists. The columns at one of the building facades were modelled using two-node beam elements with six degrees of freedom at each node. A total of 1,205 elements with

Table 3 - Material properties used in finite element analysis			
Element	Density (kg/m^3)	Elastic modulus (GPa)	Shear modulus (GPa)
Walls	1700	3	1.25
Floor, roof	700	5	2
Columns	2400	24	10

1,336 nodes and 6,210 degrees of freedom were used for the whole building. The material properties used in the analysis are presented in Table 3.

Linear-elastic static analysis was preferred over a more realistic nonlinear dynamic one. The hypothesis of linear elasticity is justified, as: (a) the objective here was to compare the behaviour of the strengthened structure with that of the unstrengthened structure, and not to carry out detailed simulations of the seismic response; and (b) cracking is the main source of nonlinearity of unreinforced masonry and the prime characteristic of the response we are interested in for the level of stresses encountered in seismic loading. Note that the analysis procedure followed herein is consistent with that employed in [30] for the study of the response of various similar old masonry structures and verified through comparison with the observed seismic damage.

The seismic action was represented as a uniformly-distributed response acceleration separately for each horizontal direction, calculated according to the Greek seismic design code. The spectral acceleration was taken equal to 0.42 g, corresponding to the combination of a ground acceleration of 0.25 g, the 5% damped spectral amplification factor and a behaviour or response modification factor of 1.5.

Strengthening of the building was taken into account by introducing uniformly-distributed FRP tendons that provided horizontal prestressing along the spandrels (Fig. 10). The prestressing forces were taken such that the resulting confinement to the masonry was equal to 15% of the masonry compressive strength (estimated to be about 2 MPa). Similar levels of lateral stress due to prestressing were shown in [30] to be quite appropriate for a number of similar masonry buildings. The FRP reinforcement areas calculated from (14) are 425 mm^2, 375 mm^2 and 210 mm^2 for GFRP, AFRP and CFRP tendons, respectively. These figures correspond to about six GFRP or five AFRP or three CFRP 1.5-mm thick and 50-mm wide strips.

Typical results for the directions and magnitudes of the principal tensile stresses obtained for both the unstrengthened and strengthened structure in the exterior walls are

Table 4 -Average ratio of the "equivalent" stress in the strengthened building to that in the unstrengthened building												
	Walls parallel to seismic action				Walls normal to seismic action				Irrespective of seismic direction			
Story	W1	W2	W3	W4	W1	W2	W3	W4	W1	W2	W3	W4
1st	0.56 / 0.68	0.20 / 0.28	0.39 / 0.43	1.62 / 1.63	0.69 / 0.80	0.70 / 0.79	0.42 / 0.37	0.44 / 0.37	0.90 / 1.02	0.71 / 0.80	0.55 / 0.54	1.65 / 1.64
2nd	0.32 / 0.44	0.20 / 0.34	0.52 / 0.77	0.45 / 0.69	0.63 / 0.88	0.69 / 1.02	0.32 / 0.50	0.38 / 0.59	0.69 / 0.95	0.69 / 1.02	0.57 / 0.88	0.50 / 0.81

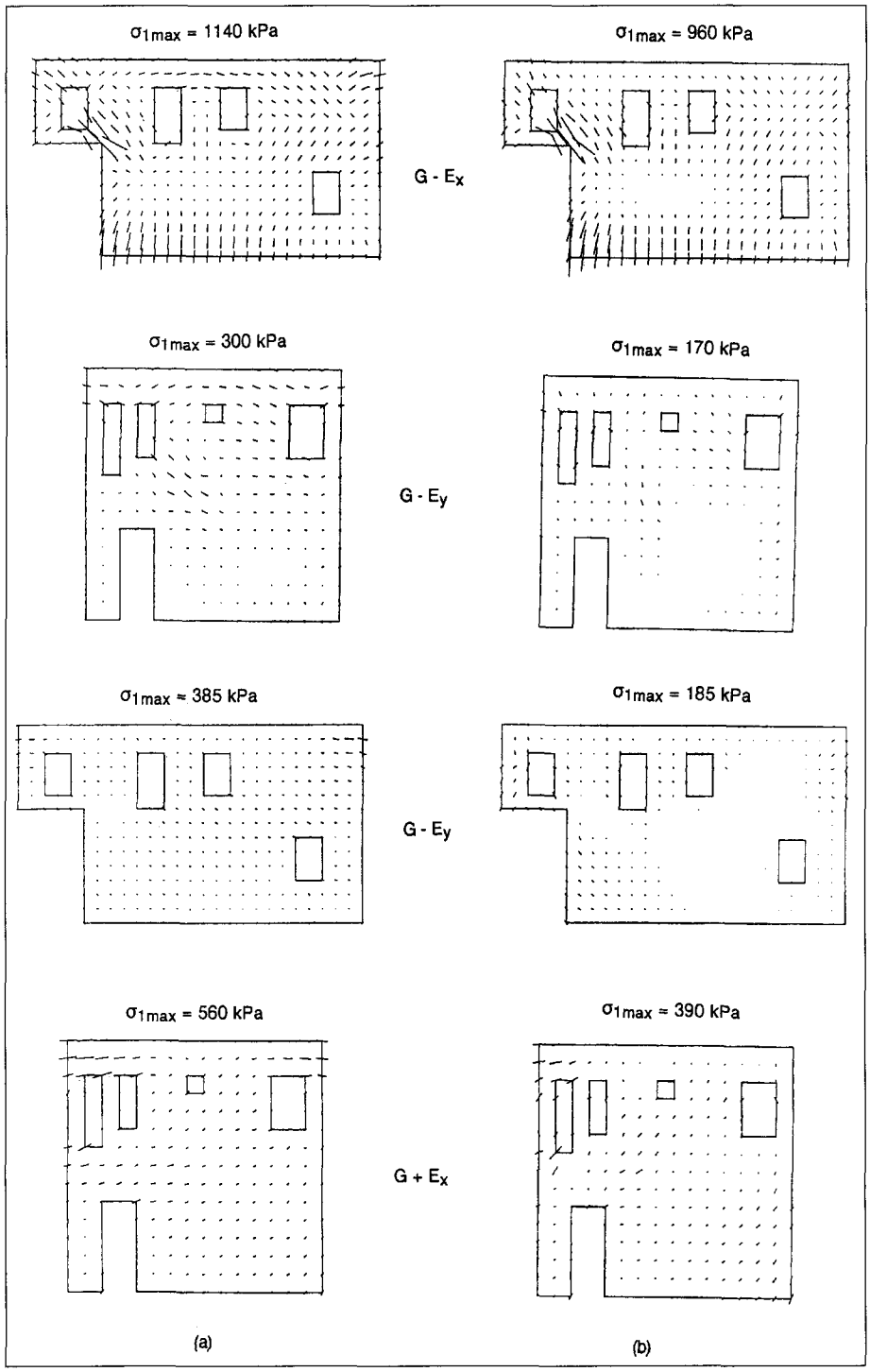

Fig. 11 – Directions and magnitudes of maximum principal tensile stresses according to FEA in walls normal and parallel to seismic action: (a) unstrengthened building; (b) strengthened building.

displayed by arrows in Fig. 11 for seismic load (E) acting either normal or parallel to the walls. Stresses shown are the maximum of the nodal stresses obtained at the external or internal surface, for seismic loads E acting simultaneously with gravity loads G, and refer to the node at the arrow midpoint. Note that the almost vertical principal tensile stresses in the basement are spurious, due to the assumed fixity of the wall at ground level.

A measure of the effectiveness of the proposed strengthening technique can be obtained by considering the proximity of the state of stress to the failure criterion in (3) over each wall and story of the building. This proximity is quantified by computing the proportionality factor σ^* such that the stress point ($\sigma^*\sigma_1$, $\sigma^*\sigma_2$) lies on the failure envelope. Hence, the scaling factor σ^* has the meaning of an "equivalent" stress, normalised with respect to its failure value. The ratio of the maximum value of σ^* at a given point (on either surface of the wall for all combinations of interest of the gravity load with the seismic action) in the strengthened building to that in the unstrengthened building provides a local measure of the effectiveness of the strengthening technique. The mean value of this ratio over each wall and each story of the building provides an average measure of the effectiveness of the intervention; this value is listed in Table 4 separately for the walls normal to the seismic action in order to show the effectiveness for the most important out-of-plane behaviour, then for those walls parallel to the seismic action for the less important in-plane behaviour, and finally independent of the direction of the wall relative to the seismic action, that is, for the most adverse direction of the seismic action. The figures in Table 4 show that the reduction in stress, in the average sense described above, may be up to approximately 10% in the first story

Table 5 - Maximum principal tensile stresses (kPa)

	Unstrengthened building					Strengthened building				
Load case	W1	W2	W3	W4a	W4b	W1	W2	W3	W4a	W4b
$G + E_x$	1140	1050	560	1060	375	970 (-15%)	970 (-8%)	390 (-30%)	1000 (-6%)	195 (-48%)
$G + E_y$	470	290	350	315	210	440 (-6%)	210 (-28%)	420 (+20%)	220 (-30%)	190 (-10%)
$G - E_x$	1110	1140	530	930	410	995 (-10%)	960 (-16%)	345 (-35%)	965 (+4%)	350 (-15%)
$G - E_y$	450	315	300	370	190	440 (-2%)	185 (-41%)	170 (-44%)	450 (+21%)	195 (+3%)

Table 6 - Representative elastic moduli and coefficients of thermal expansion		
Material	Elastic modulus (GPa)	Coefficient of thermal expansion ($\times 10^{-6}$ / °C)
GFRP	50	7
AFRP	65	-4
CFRP	140	0.5
Masonry	3	10

and 40% in the second, and the effectiveness of the proposed strengthening technique is considered to be quite satisfactory and analogous to that of the technique involving horizontal prestressing with steel tendons, *e.g.* [24].

As an alternative measure of the effectiveness of the intervention, one may consider the reduction in the maximum principal stresses. These stresses over each wall of both the unstrengthened building and the strengthened building are summarised in Table 5. The figures given in parentheses in Table 5 show that the reduction (or, in a few cases, the slight increase) in the maximum principal stresses may be up to approximately 50%, depending on the wall and the type of loading, and hence the proposed strengthening technique is considered to be effective.

7. TEMPERATURE EFFECTS

The coefficient of thermal expansion for unidirectional composites may be considerably different from that of masonry, thus leading to the development of additional stresses in both the tendons and the masonry. The magnitude of these stresses is estimated here by means of a simplified analysis. Considering a temperature change ΔT with respect to the temperature at post-tensioning in a region of the masonry where the FRP tendon area fraction is ρ_{frp}, the strain (causing stresses) in the tendons due to ΔT, $\varepsilon_{frp,\Delta T}$, can be calculated on the basis of simple force equilibrium and strain compatibility relationships. Strain compatibility yields:

$$\varepsilon_{frp,\Delta T} - \varepsilon_{w,\Delta T} = (\alpha_w - \alpha_{frp})\Delta T \quad (17)$$

where α_w and α_{frp} are coefficients of thermal expansion of the masonry and the FRP, respectively, and $\varepsilon_{w,\Delta T}$ is the strain (causing stresses) in the masonry due to ΔT. Force equilibrium in the masonry-FRP system gives:

$$\sigma_{frp,\Delta T}\,\rho_{frp} + \sigma_{w,\Delta T} = \varepsilon_{frp,\Delta T}\,E_{frp}\,\rho_{frp} + \varepsilon_{w,\Delta T}\,E_w = 0 \quad (18)$$

in which $\sigma_{frp,\Delta T}T$ and $\sigma_{w,\Delta T}$ are the stresses in the tendons and the masonry, respectively, due to ΔT, and E_{frp} and E_w are the corresponding elastic moduli. Combining (17)-(18), the following equation is obtained for $\varepsilon_{frp,\Delta T}$:

$$\frac{\varepsilon_{frp,\Delta T}}{\Delta T} = \frac{(\alpha_w - \alpha_{frp})}{\left[1 + (E_{frp}/E_w)\,\rho_{frp}\right]} \quad (19)$$

For the typical material properties of Table 6, $\varepsilon_{frp,\Delta T}$ (per °C) is plotted in Fig. 12 in terms of ρ_{frp}. It becomes clear that the additional FRP strains are negligible and almost independent of the tendon area fraction. For

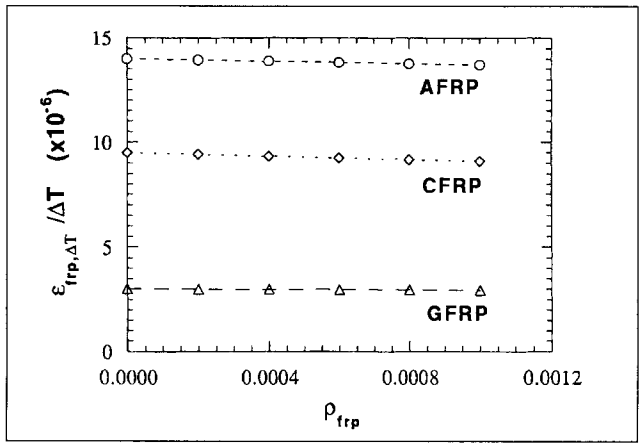

Fig. 12 – FRP tendon strains versus area fraction, due to temperature change.

instance, the rather extreme case of ΔT = 30 °C gives an additional tensile strain for CFRP tendons equal to 0.0003, which is less than 5% of the CFRP strain due to prestressing. The corresponding values for AFRP and GFRP are less than 2%.

The expression obtained from (18) for the strain in the masonry due to ΔT is:

$$\varepsilon_{w,\Delta T} = -\varepsilon_{frp,\Delta T}\frac{E_{frp}}{E_w}\rho_{frp} \quad (20)$$

which yields negligible values.

In summary, the stresses and the associated strains resulting from temperature variations are small in both the tendons and the masonry, and hence, temperature effects are not expected to impair the load-bearing capacity of the system.

8. DISCUSSION AND CONCLUSIONS

In the present study, the authors propose the application of composite post-tensioned external tendons for the reversible consolidation and strengthening of historical masonry structures. These materials offer excellent physical and mechanical properties, are lightweight and insensitive to corrosion, and can be easily applied in a reversible manner as circumferential externally attached tendons in a colour matching that of the external surface of the structure. The proposed concepts for the application and attachment of post-tensioned FRP ties are developed with the objectives of providing horizontal confinement and minimising anchor lengths. The proportioning of the strengthening can be accomplished on the basis of the general design procedure proposed herein, which is applicable to any type of (isotropic) masonry structure and material.

Analytical solutions for simple load cases on simple structures and finite element analysis results show that the effectiveness of the strengthening technique with FRP tendons, quantified in terms of increased resistance to gravity and lateral loads, is quite satisfactory. Also, the simplified analysis of temperature effects on the FRP-masonry system shows that the additional stresses due to thermal

mismatch of the two materials are very low.

Other considerations, such as creep of both the FRP and the masonry, are not specifically accounted for in the present study. Creep of both unidirectional composites (except for AFRP) and old masonry loaded at low prestress levels (on the order of 10% of their compressive strength) is expected to be negligible; however, precise calculations of creep effects can easily be performed, based on realistic creep models for composites (*e.g.* Findley's law) and masonry materials. Another issue of importance to structures located in seismic areas is that FRPs are rather brittle, but given the large failure strains of the materials (approximately 1.5-4%), such a brittleness is not necessarily of concern in masonry consolidation applications. Lastly, ultraviolet radiation may cause problems to exposed FRP tendons, so the use of protective additives in the matrix or thin coatings may be necessary.

Overall, it is shown that the FRP-strengthening technique, as applied here to historical masonry structures (especially with CFRP materials), appears to provide a simple, efficient and effective method for the structural preservation of our architectural heritage.

9. ACKNOWLEDGEMENTS

This research was partially supported by the Hellenic General Secretariat for Research and Technology and by the Hellenic Ministry of Education. The authors wish to thank Mr. I. Argyropoulos and Dr. F. Karantoni for their invaluable assistance in obtaining some of the finite element analysis results.

10. REFERENCES

[1] Charter of Venice, 'Decisions and resolutions', in Proceedings of the 2nd International Congress for Architects and Technicians of Historic Monuments, Venezia, 1964, **5**, 25-31 (in French).

[2] United Nations Development Program / United Nations Industrial Development Organization, 'Building Construction Under Seismic Conditions in the Balkan Region, Vol. 6: Repair and Strengthening of Historical Monuments and Buildings in Urban Nuclei' (UNDP/UNIDO Proj. RER/79/015 Vienna, 1984).

[3] Wenzel, F., 'On the structural repair of masonry', in 'Structural Repair and Maintenance of Historical Buildings' (Computational Mechanics Publications, Southampton, 1989) 83-94.

[4] Miltiadou, A. and Delinicola, E., 'Earthquake resistant preventive measures to consolidate a historical rampart' in Proceedings of the 8th European Conference on Earthquake Engineering, Lisbon, **11.2** (1986) 41-48.

[5] Bohn, K., 'Strengthening of Pisa Tower by external post-tensioning', in 'Structural Preservation of the Architectural Heritage', Proceedings of IABSE Symposium, Rome, 1993, 715-716.

[6] Croci, G., 'Structural aspects in restoring monuments', in *Ibid.*, 13-28.

[7] Zurli, F. and Viola, R. M., 'Damage and repair of the St. Charles Basilica in Rome', in *Ibid.*, 417-423.

[8] Triantafillou, T. C. and Fardis, M. N., 'Advanced composites for strengthening historic structures', in *Ibid.*, 541-548.

[9] Hull, D., 'An Introduction to Composite Materials' (Cambridge University Press, 1981).

[10] Preis, L. and Bell, T. A., 'Fibreglass tendons for post-tensioning concrete bridges', Transportation Research Record 1118 (National Research Council, Washington, D.C., 1986) 77-82.

[11] Imperial College of Science and Technology, 'Engineering Applications of Parafil Ropes', Proceedings of a Symposium, London, 1988.

[12] Tanigaki, M., Okamoto, T., Tamura, T., Matsubara, S. and Nomura, S., 'Study of braided aramid fibre rods for reinforcing concrete', in Proceedings of the 13th IABSE Congress, Helsinki, 1988, 15-20.

[13] Gerritse, A. and Werner, J., 'Arapree, a non-metallic tendon', in 'Advanced Composite Materials in Civil Engineering Structures', ASCE Spec. Conf., Las Vegas, 1991, 143-154.

[14] Kakihara, R., Kamiyoshi, M., Kumagai, S. and Noritake, K., 'A new aramid rod for the reinforcement of prestressed concrete structures', in *Ibid.*, 132-142.

[15] Zoch, P., Kimura, H., Iwasaki, T. and Heym, M., 'Carbon fibre composite cables - a new class of prestressing members', in Proceedings of the 70th TRB Annual Meeting, Washington D.C., 1991.

[16] Koga, M., Okano, M., Sakai, H., Kawamoto, Y. and Yagi, K., 'Application of a tendon made of CFRP rods to a post-tensioned prestressed concrete bridge', in 'Advanced Composite Materials in Bridges and Structures', Proceedings of the 1st International Conference, Sherbrooke, Canada, 1992, 405-414.

[17] Machida, A., Editor, 'State-of-the-art Report on Continuous Fiber Reinforcing Materials' (Japan Society of Civil Engineers, 1993).

[18] Nanni, A. and Dolan, C. W., Editors, 'Fiber-reinforced-plastic reinforcement for concrete structures', Proceedings of International Symposium (ACI SP-138, Detroit, 1993).

[19] ACI Committee 440, 'State-of-the-Art Report on FRP Reinforcement' (ACI, Detroit, 1996).

[20] Plevris, N. and Triantafillou, T., 'FRP-reinforced wood as structural material', *ASCE J. Mater. Civ. Engrg.* **4** (3) (1992) 300-317.

[21] Triantafillou, T. C. and Deskovic, N., 'Prestressed FRP sheets as external reinforcement of wood members', *ASCE J. Struct. Engrg.* **118** (5) (1992) 1270-1284.

[22] Schwegler, G., 'Masonry construction strengthened with fibre composites in seismically endangered zones', in Proceedings of the 10th European Conference on Earthquake Engineering, Vienna, 1994.

[23] Triantafillou, T. C. and Fardis, M. N., 'Strengthening of historic masonry structures with fibre reinforced plastic composites', in 'Dynamics, Repairs & Restoration', Proceedings of the 4th International Conference on Structural Studies of Historical Buildings (STREMA 95), Chania, Greece, May, 1995, 129-136.

[24] Karantoni, F. V., Fardis, M. N., Vintzeleou, E. and Harisis, A., 'Effectiveness of seismic strengthening measures', in 'Structural Preservation of the Architectural Heritage', Proceedings of IABSE Symposium, Rome, 1993, 549-556.

[25] Ottosen, N., 'A failure criterion for concrete', *ASCE J. Engrg. Mech.* **103** (4) (1977) 527-535.

[26] Ganz, H. R. and Thuerliman, B., 'Design of masonry walls under normal force and shear', in Proceedings of the 8th International Brick/Block Masonry Conference, Dublin, 1988, 1447-1457.

[27] Koenig, G., Mann, W. and Oetes, A., 'Untersuchungen zum verhalten von mauerwarksbauten unter erdbeben eienwirkung', Koenig und Heunisch, Frankfurt, 1988.

[28] Dialer, C., 'Some remarks on the strength and deformation behaviour of shear stressed masonry panels under static monotonic loading', in Proceedings of the 9th International Brick/Block Masonry Conference, Berlin, 1991, 276-283.

[29] FIP Commission on Prestressing Materials and Systems, 'High-strength Fibre Composite Tensile Elements for Structural Concrete, State-of-Art-Report, 1992.

[30] Karantoni, F. V. and Fardis, M. N., 'Computed versus observed seismic response and damage of masonry buildings', *ASCE J. Struct. Engrg.* **118** (7) (1992) 1804-1821.